JOURNAL OF IRON AND STEEL RESEARCH, INTERNATIONAL. 2016, 23(6): 547-552

Influence of Residual Stress on Shape of Heavy-gauge, High-strength Steel Caused by Cooling Process after Hot Rolling

Shui-ze WANG[1,2], Yong-lin KANG[1], Guo-ming ZHU[1], Wen LIANG[2]
(1. School of Materials Science and Engineering, University of Science and Technology Beijing, Beijing 100083, China;
2. Research and Development Center, Wuhan Iron & Steel (Group) Co., Ltd., Wuhan 430080, Hubei, China)

Abstract: The cooling process following hot rolling has a significant effect on the shape quality of a hot-rolled strip. The temperature and stress fields in the cooling process for a 14 mm thick strip with yield strength of 500 MPa grade were analyzed by the finite element method and actual test data, and the relationship between residual stress and shape defects was described. Subsequently, the small-crown rolling process and the coil slow cooling process were investigated. The results indicate that these processes improved the shape quality of the final product significantly.
Key words: heavy-gauge; high-strength steel; non-uniform cooling; residual stress; buckling deformation

The cooling process following hot rolling of a heavy-gauge, high-strength steel strip is an important post-processing step for the final hot-rolled product. The cooling process influences the mechanical properties and shape quality of the product directly. The improvements in temperature calculations and the control model[1-3] resulted in higher temperature control precision of the strip. Specifically, there were significant improvements in the temperature control precision of the finish rolling temperature and the coiling temperature. However, the temperature control mode could only control the temperature fluctuations in the length direction. The fluctuation in the thickness and width directions could not be controlled effectively. Ginzburg et al.[4] proposed that the temperature gradient in the width and thickness directions of the strip is the main cause of side waves, bow waves, and other forms of shape defects. During the actual production process, researchers also found that the shape detected online is different from the offline observation results. This was especially true for heavy-gauge, high-strength steel. The flatness of the strip tested online was good. However, warping phenomenon was observed when the strip was slitted[5-7]. Studies suggested that the residual stress caused by non-uniform cooling is the direct cause of the warping problem. In this study, the influence of non-uniform cooling on residual stress and flatness of heavy-gauge, high-strength steel was analyzed using the finite element simulation and actual test data. Additionally, it is proposed that small-crown rolling and coil slow cooling improve the shape quality of the final hot-rolled product.

1 Experimental Method

1.1 Finite element simulation of cooling process

1.1.1 Physical model and element meshing

The thickness, width, and length of the strip to be simulated were 14, 1600, and 2000 mm, respectively. The model was split by an 8-noded hexahedrons element. The Cartesian coordinate system was used for the finite element simulation, where the X, Y, and Z directions represent the width, thickness, and length of the workpiece, respectively.

1.1.2 Thermophysical parameters of the material

High strength Q460 steel was the material selected in this study. The thermal diffusivity and specific heat of the material were measured by the laser thermal conductivity meter and high-temperature

Foundation Item: Item Sponsored by National Natural Science Foundation of China (U1460101)
Biography: Shui-ze WANG, Doctor Candidate; **E-mail**: wangshuize-316@163.com; **Received Date**: November 24, 2015
Corresponding Author: Yong-lin KANG, Doctor, Professor; **E-mail**: kangylin@ustb.edu.cn

differential scanning calorimeter, respectively. Additionally, the thermal expansion coefficient at different temperatures was obtained by thermal simulation tests. The thermophysical parameters of the material are listed in Table 1.

Table 1 Thermophysical parameters of Q460 steel

Temperature/℃	Heat conductivity/ ($W \cdot m^{-1} \cdot K^{-1}$)	Specific heat/ ($J \cdot kg^{-1} \cdot K^{-1}$)	Linear expansivity/ ($10^{-6} K^{-1}$)
50	55.9	458	12.64
100	54.3	478	12.83
300	45.7	582	13.57
500	37.0	711	14.28
700	30.6	1025	14.61
900	27.5	612	11.96

1.1.3 Boundary conditions and initial conditions

The finish rolling and coiling temperatures of the strip were 880 ℃ and 640 ℃, respectively. The cooling process was divided into four steps, as shown in Fig. 1. Step 1 involved an air cooling process in which the main heat-transfer modes were thermal radiation and heat convection[8-11]. Based on the rolling speed of the strip, the duration of the air cooling process was approximately 2 s. Step 2 was a water cooling process. Herein, the convection heat-transfer coefficient was calculated using the regression equation in Eq. (1); the holding time was approximately 10 s. Step 3 was also an air cooling process, where the holding time was about 10 s. Step 4 was a coil cooling process in which the heat exchange process was slower[12-14]. In this paper, a simplified method was used to simulate the temperature drop of the coil and homogenization process of temperature by considering a relatively lower heat transfer coefficient.

$$h_w = \frac{1.13\times10^6\overline{\omega}^{0.355}}{(T-T_w)} \cdot \left[\frac{(2.5-1.5\log T_w)D}{P_L P_C}\right]^{0.645} \quad (1)$$

where, $\overline{\omega}$ is the current density, and generally can be 100 $m^3 \cdot min^{-1} \cdot m^{-2}$; T_w is the temperature of water, ℃; D is the nozzle diameter, m; and P_L and P_C are the nozzle spacing along the rolling and vertical rolling directions, respectively, m.

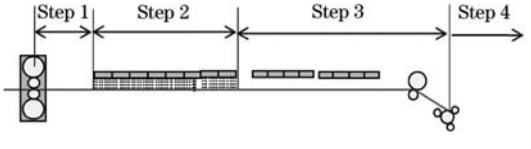

Fig. 1 Cooling process of hot strip after hot rolling

1.1.4 Method of calculation

To simplify the calculation, the initial temperature of the strip was assumed to be uniform, the initial stress was assumed to be zero, and the influence of phase transformation on temperature and stress was ignored. The temperature and stress fields of the strip in the laminar cooling process were calculated using the thermal coupling calculation module of the commercial finite element software ANSYS/LS-DYNA.

1.2 Residual stress test

Residual stress was measured by a drilling method shown in Fig. 2, and the model of the test device was ASMB2-8. The measured points are shown in Fig. 3. A total of seven points along the width direction were measured, in which points 1 and 7 were 10 mm away from the edge. The other points were spaced equally.

Fig. 2 Drilling test method

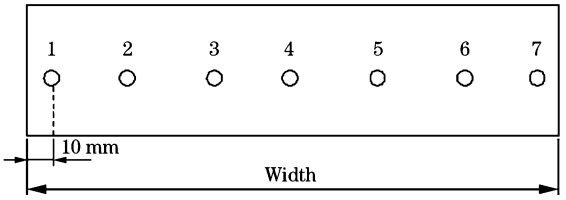

Fig. 3 Distribution of measured points

1.3 Measurement of buckling deformation

Using plasma cutting, the sample was divided into five parts along the width direction, as shown in Fig. 4. Then, the cut plate was placed on the hori-

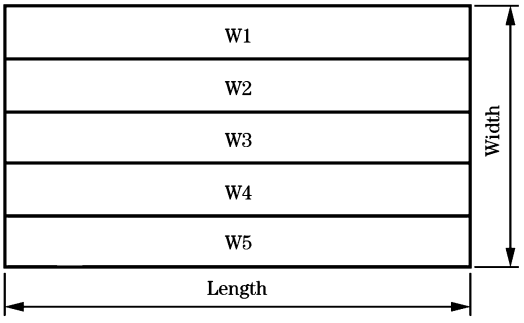

Fig. 4 Cutting scheme

zontal platform to measure the buckling deformation value, as shown in Fig. 5.

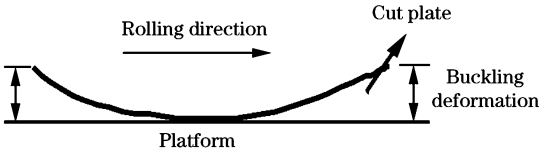

Fig. 5 Method for buckling deformation measurement method

1.4 Experiment to improve shape quality

1.4.1 Small-crown rolling experiment

The crown adjustment experiment was carried out to analyze the influence of the crown on the flatness of the strip and to improve the shape quality of the final product. The target crown values were set as shown in Table 2.

Table 2 Target crown values

Scheme	A	B	C
Crown value/μm	40	80	120

1.4.2 Coil slow cooling experiment

The coil cooling experiment was performed to analyze the influence of the coil cooling model on the shape quality of final product. The experimental scheme is shown in Table 3.

Table 3 Coil cooling scheme

Scheme	D	E
Cooling mode	Air cooling	Temperature-keeping cover over the coil for 120 h

2 Results and Discussion

2.1 Analysis of temperature evolution during cooling process after hot rolling

Fig. 6 illustrates the temperature evolution of the surface and core of the strip during the laminar cooling process. As indicated in Fig. 6, the surface temperature dropped rapidly after the strip entered into the water cooling zone. This resulted in a certain temperature gradient between the surface and core. The maximum temperature gradient had reached 82 ℃ when the water cooling process was completed. In the subsequent air cooling process, the temperatures of the surface and core were consistent.

The temperature evolution of the edges and middle parts of the strip during the laminar cooling process is detailed in Fig. 7. As observed from Fig. 7, the temperature at the middle part and edges of the

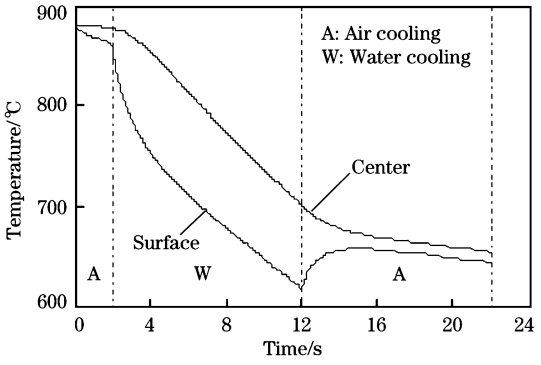

Fig. 6 Temperature curve of the surface and center parts of the strip

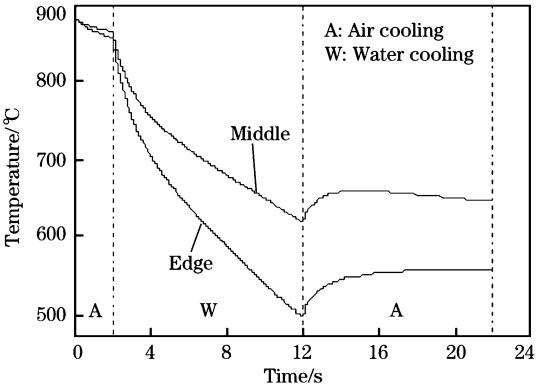

Fig. 7 Temperature curve of the edges and middle parts

strip dropped rapidly after the strip entered into the water cooling zone. The cooling rate at the edges was faster than that at the middle part. When the water cooling process was completed, the maximum temperature difference reached 120 ℃. In the subsequent air cooling process, the temperature difference was reduced. The temperature distribution curve along the width direction of the strip before coiling is illustrated in Fig. 8. As shown in Fig. 8, there was a sharp drop in the temperature at the edges of the strip and

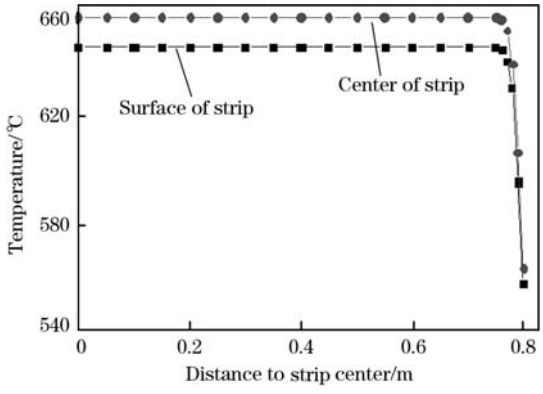

Fig. 8 Temperature distribution curve along the width direction before coiling

the maximum temperature difference reached 70 ℃. The temperature distribution of the strip before coiling, as measured by an infrared thermal imager, is shown in Fig. 9. It can be seen that the measured values were close to the calculated values. This implies that the temperature field calculated by a numerical simulation method had certain reliability. As the temperature field calculation was the basis for the subsequent stress calculation, the reliability of the temperature calculation can ensure the reliability of the stress calculation to a certain extent.

The temperature difference between the middle part and edges of the strip reduced gradually after coiling and finally tended to be the same. The simulation results are presented in Fig. 10. The measurement results detailed in Fig. 11 indicate that when the coil was cooled to 140 ℃, the temperature difference between the middle part and edges of the strip reduced from 70 to 20 ℃.

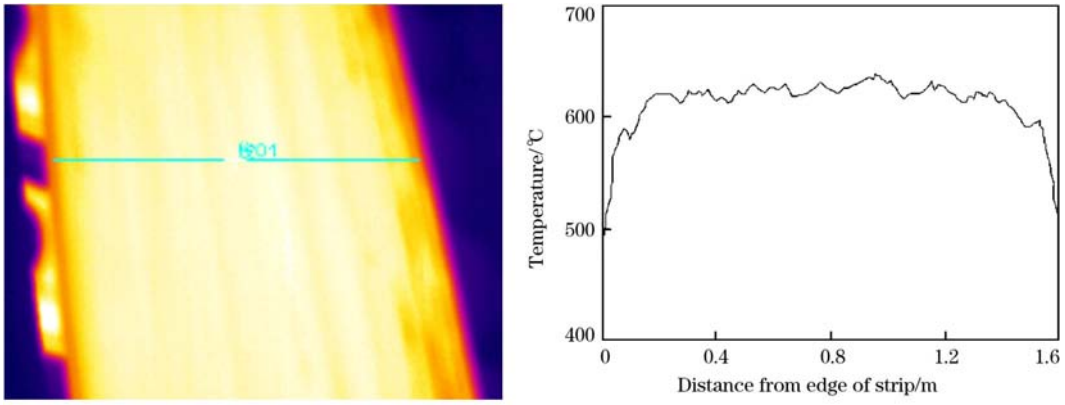

Fig. 9 Temperature distribution before coiling measured by infrared thermal imager

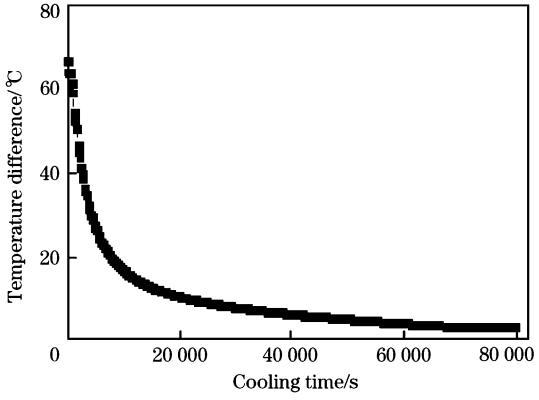

Fig. 10 Temperature difference calculated between the middle part and edges of the strip

2.2 Analysis of stress evolution during cooling process after hot rolling

The evolution of internal stress at the edges and middle parts of the strip during the cooling process is depicted in Fig. 12. When the strip entered into the laminar cooling zone, there was a certain temperature gradient between the middle part and the edges of the strip due to non-uniform cooling; this resulted in the phenomenon where the shrinkage in the strip was inconsistent along the width direction. At first, the edges were subjected to tensile stress, while the middle part was subjected to compressive

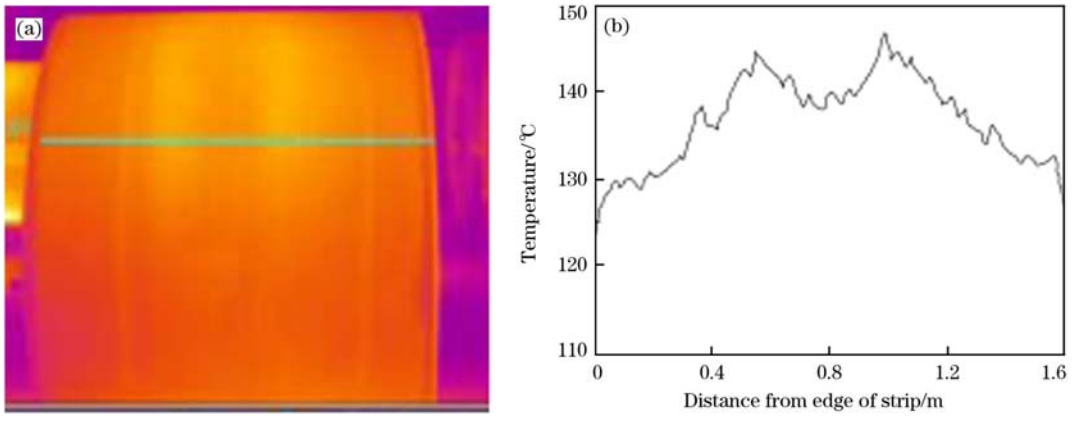

Fig. 11 Measured surface appearance (a) and temperature distribution (b) of the coil

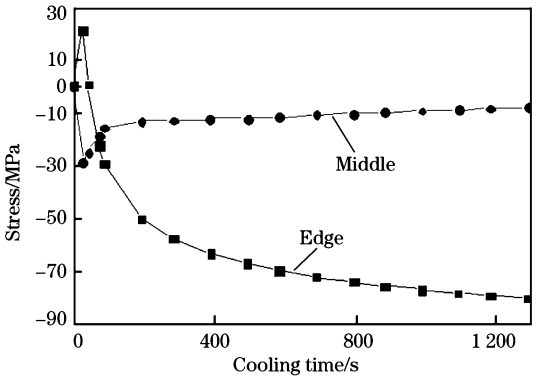

Fig. 12 Stress evolution at the middle part and edges of the strip during cooling process

stress. This led to a faster temperature-drop at the edges. In the subsequent air cooling process, the cooling rate at the middle part exceeded the cooling rate at the edges gradually. This led to a greater contraction at the middle part compared with the edges. The tensile stress at the edges decreased gradually and it even turned into compressive stress. The compressive stress at the middle part also decreased gradually.

The stress distribution along the width direction is shown in Fig. 13. It can be seen that the distribution of the residual stress was non-uniform in the thickness and width directions. There was a large compressive stress at the edges; this typically caused the shape defects in the strip after the cooling process.

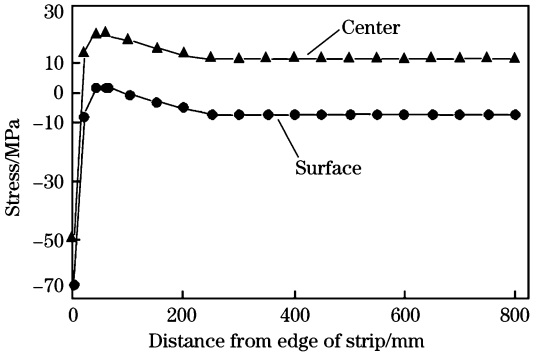

Fig. 13 Distribution of residual stress

2.3 Analysis of influence of residual stress on shape quality

The residual stress of the strip was measured by the drilling method. The measured points are shown in Fig. 3, and the measured results are depicted in Fig. 14. It can be observed that the edges of the strip were subjected to compressive stress and the middle part was subjected to tensile stress. The measured results were in agreement with the calculated results.

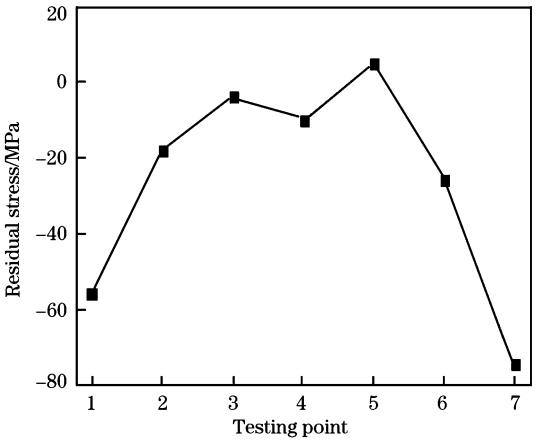

Fig. 14 Measured residual stress distribution

The plate with a thickness, width, and length of 14, 1600, and 2000 mm, respectively was cut. The methods of cutting and measuring are shown in Figs. 4 and 5, and the measured results are listed in Table 4. It was observed that the buckling deformation defect at the edges was more prominent than that at the middle part of the strip. The buckling deformation value of the edge part was 3—4 times the deformation value of the middle part; this was directly related to the relatively larger compressive stress at the edges.

Table 4 Buckling deformation value of the sample

Position	W1	W2	W3	W4	W5
Deformation value/mm	9.2	2.5	1.8	3.0	8.5

2.4 Shape quality improvement

2.4.1 Small-crown rolling process

According to the above mentioned analysis, the problems of shape defects were particularly prominent at the edges when the strip was cooled by laminar flow. To control the shape quality of the final product, flatness target values at the exit of the final mill were set as a micro middle wave to compensate for the change in the shape of the strip after the cooling process[15]. Herein, the target-crown adjustment was carried out to improve the shape quality of the final product, given the relationship between the crown and flatness. The experimental scheme is presented in Table 2. The testing sample was cut and measured using the method detailed in Figs. 4 and 5, and the measured results are shown in Table 5. It was noted that the buckling deformation defect at the edges improved evidently with scheme A from Table 5. The small-crown rolling process had a cer-

Table 5 Measured values of buckling deformation for schemes A, B and C

Position	W1	W2	W3	W4	W5
Scheme A	4.3	2.3	1.5	3.2	3.6
Scheme B	9.6	2.1	1.2	4.8	8.5
Scheme C	13.2	6.3	1.0	4.6	12.5

tain effect on solving the problem of the buckling deformation defect of the final product.

2.4.2 Coil slow cooling process

The residual stress caused by inhomogeneous cooling after hot rolling is one of the main reasons for the buckling deformation defect. The coil slow cooling process can play a crucial role in the stress-relieving heat treatment, such that it improves the shape quality of the final product. The experimental scheme is shown in Table 3. The sample was cut and measured using the method detailed in Figs. 4 and 5, and the measured results are indicated in Table 6. It can be seen that the problem of the buckling deformation defect improved significantly when the coil adopted the slow cooling process.

Table 6 Measured values of buckling deformation for schemes D and E

Position	W1	W2	W3	W4	W5
Scheme D	14.2	4.5	2.3	3.8	8.6
Scheme E	2.8	1.0	1.0	1.4	2.2

3 Conclusions

(1) A numerical simulation method was used to analyze the evolution of the temperature and stress field of the strip during the cooling process. The simulation results suggest that the edge of the strip was subjected to large compressive stress due to non-uniform cooling. The measured results of residual stress followed the same distribution law as the numerical simulation results. The results indicate that the compressive stress at the edges of the strip was the main reason for buckling deformation.

(2) The results of the crown adjustment experiment indicate that the small-crown rolling process can compensate for the heterogeneous distribution of stress in the cooling process; this, in turn, can improve the shape quality of the final product.

(3) The results of the coil slow cooling experiment indicate that the heat preservation process for the coil, which plays a similar role in stress-relieving heat treatment, can improve the shape quality of the final product.

References:

[1] H. B. Xie, X. H. Liu, G. D. Wang, Z. P. Zhang, J. Iron Steel Res. Int. 13 (2006) No. 1, 18-22.
[2] J. Wang, G. D. Wang, X. H. Liu, J. Iron Steel Res. Int. 11 (2004) No. 5, 13-17.
[3] D. H. Zhang, N. Zhou, B. X. Wang, M. Zhang, J. Iron Steel Res. Int. 17 (2010) No. 1, 18-21.
[4] V. B. Ginzburg, High Quality Steel Rolling Theory and Practice, Metallurgical Industry Press, Beijing, 2002.
[5] C. X. Xiao, Baosteel Technology (2000) No. 3, 1-5.
[6] Q. L. Cui, M. Zhao, G. Yuan, X. H. Liu, G. D. Wang, J. Iron Steel Res. 19 (2007) No. 9, 21-23.
[7] Z. Cai, G. D. Wang, X. H. Liu, K. Zhao, J. G. Yuan, Iron and Steel 35 (2000) No. 6, 33-36.
[8] X. H. Cai, Z. A. Luo, G. D. Wang, X. H. Liu, J. Iron Steel Res. Int. 11 (2004) No. 1, 26-28.
[9] W. Yu, X. J. Lu, Y. L. Chen, B. Bai, Iron and Steel 46 (2011) No. 4, 44-45.
[10] S. J. Lu, Wide and Heavy Plate 9 (2003) No. 6, 34-35.
[11] Y. P. Su, Q. Yang, A. R. He, X. D. Wang, H. T. Bian, Steelmaking 43 (2008) No. 5, 55-59.
[12] J. F. Chen, Z. D. Liu, H. Dong, Y. Gan, Iron and Steel 39 (2004) No. 10, 40-44.
[13] J. Q. Sun, J. C. Lian, J. Yanshan Univ. 22 (1998) No. 3, 222-223.
[14] J. Q. Sun, J. H. Sun, B. Wu, J. C. Lian, J. Iron Steel Res. Int. 12 (2005) No. 2, 33-36.
[15] X. D. Wang, F. Li, Q. Yang, A. R. He, Applied Mathematical Model 37 (2013) 586-609.